Surface Science 646 (2016) 204–209

Contents lists available at ScienceDirect

Surface Science

journal homepage: www.elsevier.com/locate/susc

Orientational anisotropy and interfacial transport in polycrystals

M.M. Moghadam, J.M. Rickman *, M.P. Harmer, H.M. Chan

Department of Materials Science and Engineering, Lehigh University, Bethlehem, PA 18015, United States

ARTICLE INFO

Available online 20 June 2015

Keywords:
Diffusion
Computer simulation
Grain boundary

ABSTRACT

Interfacial diffusion is governed to a large degree by geometric parameters that are determined by crystallographic orientation. In this study, we assess the impact of orientational anisotropy on mass transport at internal interfaces, focusing on the role of preferred crystallographic orientation (i.e., texture) on mass diffusion in a polycrystal. More specifically, we perform both numerical and analytical studies of steady-state diffusion for polycrystals having various grain-orientation distributions. By relating grain misorientation to grain-boundary energies and, via the Borisov relation, to the diffusivity, we link microstructure variability to kinetics. Our aim is to correlate shape features of the orientation distribution, such as the location and shapes of peaks, with the calculated effective diffusivity. Finally, we discuss the role of crystallographic constraints, such as those associated with grain junctions, in determining the effective diffusivity of a polycrystal.

1. Introduction

Many studies have established that atomic diffusion at interfaces depends, in general, on geometric parameters that are determined by the orientation of the interface, local atomic coordination, etc. For example, Ayrault and Ehrlich demonstrated that there is an orientational anisotropy in surface self-diffusion for Rh [1], while early work on the surface self-diffusion of Pt atoms showed that diffusion mechanisms depended on surface orientation for channeled surfaces [2,3]. In the case of internal interfaces, such as grain boundaries, boundary orientation also dictates the observed interfacial diffusivity. The orientational anisotropy of boundary transport was studied in early work by Turnbull and Hoffman in which Ag self-diffusion in tilt grain boundaries was shown to depend on crystal misorientation [4,5]. Somewhat later, Herbeuval *et al.* [6] also noted an orientational anisotropy in measured self-diffusion rates of aluminum for various tilt boundaries.

From the foregoing discussion, it is evident that the transport behavior for a material comprising many interfaces, such as grain boundaries in a polycrystal, will necessarily involve a complex interplay among the disparate diffusive paths connecting these interfaces. For this reason, most tractable descriptions of grain-boundary (GB) diffusion in polycrystals make the simplifying assumption that all boundaries have the same diffusivities. However, given the inherent richness of a typical GB character distribution (i.e., a summary of the observed grain orientations and related macroscopic degrees of freedom) [7], there is, in fact, a spectrum of boundary diffusivities, and it is an open question as to how these diffusivities conspire to determine the effective transport behavior of a polycrystal. In one limiting case, namely that corresponding to highly textured materials in which grain orientations are non-random, a relatively small subset of crystallographic orientations dictates observable, anisotropic properties [8,9]. Such textures arise, for example, when a metal is plastically deformed in a forming operation.

Some workers have begun to link GB variability (i.e., boundaries having a spectrum of boundary activation energies and, hence, diffusivities) to the effective diffusivity in polycrystals in several studies. For example, Schuh and coworkers [10] examined effective medium approximations for the effective diffusivity in simplified models of heterogeneous GB networks. Similarly, Li and Holland [11] investigated a model having two distinct GB diffusivities to assess the roles of network topology and boundary character in determining the collective diffusion response of the system. Most recently, Mohebi-Moghadam *et al.* [12] studied the impact of GB variability on diffusion in a polycrystal by obtaining an effective diffusivity as a function of temperature for different microstructures using multi-state models. In most of the aforementioned studies simplifying assumptions for the grain-orientation probability density function (pdf) were employed, resulting in a spectrum of boundary diffusivities comprising one or two states [13]. While these investigations provide an important link between boundary structure and interfacial transport, it is also desirable to connect the effective diffusivity to GB character distributions that reflect the microstructural complexity and preferred grain orientations in many materials.

Several models may be employed to represent the distribution of grain orientations and associated misorientations in a polycrystal. For example, for the case of randomly misoriented grains, each grain assumed to have cubic symmetry, Mackenzie deduced the orientational pdf for grain misorientation [14,15]. This pdf highlights the relative importance of high-misorientation boundaries up to a cutoff angle of

* Corresponding author.
E-mail address: jmr6@lehigh.edu (J.M. Rickman).

http://dx.doi.org/10.1016/j.susc.2015.06.011
0039-6028/

approximately $\pi/3$ and serves as a benchmark for other distributions. In reality, in most polycrystalline materials, the grains are not randomly distributed and the grain-orientation pdf often exhibits peaks at particular orientations. In some cases, such as the design of transformer steels and polycrystalline superconductors, texture may be engineered so as to improve performance [16].

In this paper, we consider the impact of texture on GB transport in polycrystals. In doing so, we highlight the role of specific grain orientations or a range of orientations on the effective diffusivity of the system. Our approach is fairly general in that we consider generic, simplified grain-orientation pdfs and explore the consequences of orientational anisotropy on GB diffusion. This paper is organized as follows. In Section 2, we outline the simulation methodology and numerical calculation of an effective diffusivity in a polycrystal having a distribution of GB diffusivities. In Section 3, we present our simulation results and a comparison with effective-medium theory. Section 4 contains a discussion and our conclusions.

2. Simulation methodology

We employ a methodology to model GB diffusion that is described in an earlier publication [12] and adapted for our purposes here. A two-dimensional model is used here to approximate real polycrystals, although there will obviously be some differences between two- and three-dimensional systems. More specifically, we simulate steady-state GB diffusion on a square lattice with a GB network modeled as a centroidal Voronoi tessellation comprising 100 generators [17]. While the usual Voronoi tessellation [18] is based on generators that are randomly distributed in space, the centroidal Voronoi tessellation results from generators that are the mass centroids of the coalesced grains and has the virtue of producing a fairly equiaxed microstructure. This system is placed in a computational cell having dimensions $\ell \times \ell$, as shown in Fig. 1, and serves as a prototype for transport in polycrystalline materials.

The orientation, ϕ, of a particular grain is taken to be a continuous random variable drawn from a probability density function (PDF), $p(\phi)$, that we will refer to as a grain-orientation pdf. To describe polycrystals with various textures, we consider two grain-orientation PDFs, namely the Gaussian peaked at $\phi^{'}$ having a width σ and given by

$$p(\phi) = \frac{1}{\sqrt{2\pi}\sigma}\ exp\left[-\frac{\left(\phi-\phi^{'}\right)^2}{2\sigma^2}\right], \tag{1}$$

and the double-peaked Gaussian

$$p(\phi) = \frac{1}{(1+\chi)\sqrt{2\pi}\sigma}\left\{exp\left[-\frac{\left(\phi-\phi^{'}\right)^2}{2\sigma^2}\right] + \chi exp\left[-\frac{\left(\phi-\phi^{'}-\Delta\right)^2}{2\sigma^2}\right]\right\}, \tag{2}$$

the latter with peaks separated by Δ and having a relative peak height χ. Clearly, the parameter σ controls the width of each Gaussian. In practice, we truncate these densities to define a finite range for ϕ by imposing the restriction that $0 \le \phi \le \pi/2$. This truncation will change the normalization in Eq. (2); however, for $\phi^{'}$ away from 0 and $\pi/2$ and σ small, this correction is immaterial. To sample from these distributions, we use a transformation of variables for uniform deviates to generate the single Gaussian (Eq. (1)) [19] and, for the double-peaked Gaussian (Eq. (2)), we employ the rejection method [20].

Once grain orientations have been assigned randomly in space, the misorientation, ψ, associated with each GB can be determined and, from this information, the corresponding GB energy, γ, and the GB diffusivity, D_{GB}, are also calculated. More specifically, for two grains having orientations ϕ_1 and ϕ_2 meeting at a particular GB, $\psi = |\phi_1 - \phi_2|$. The dependence of γ on ψ is expected to follow the Read–Shockley model for the case of low-angle boundaries [21,22] (i.e., small ψ). For arbitrary misorientations there are approximate descriptions of GB energetics [23–25] and, for simplicity, we have adopted the Van Siclen expression [24] given by

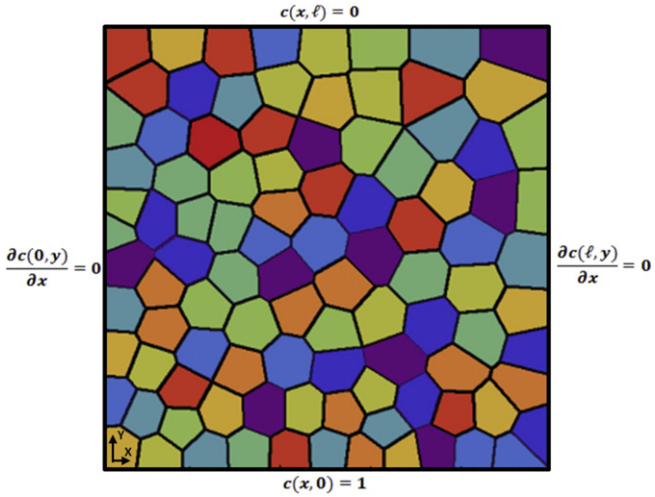

Fig. 1. A schematic of the simulation cell showing the location of the applied boundary conditions and the underlying simplified grain-boundary geometry, a centroidal Voronoi tessellation.

$$\gamma(\psi) = \gamma_0 sin(2\psi) \tag{3}$$

for $0 \le \psi \le \pi/2$. γ_0 is evidently the maximum GB energy corresponding to $\psi = \pi/4$. This expression is clearly an oversimplification that neglects, to a first approximation, the orientation of the local GB plane, θ_B. This simplification is consistent with other two-dimensional models of GB energetics [24] and grain growth [23]. To incorporate other GB degrees of freedom in this description, one can generalize Eq. (3) by construction of a GB energy, $\gamma(\theta_B - \phi_1, \theta_B - \phi_2)$, that reflects the dependence of the energetics on θ_B. (We will discuss this further in the Conclusions.) Finally, we note that, due to the crystallographic constraint that grains meet at triple junctions, the distribution of misorientations, and therefore GB energies is, however, not strictly random in space. This issue will be discussed further later in this paper.

The diffusivity, $D(\vec{r})$, for this system is taken to be an isotropic field that depends on $\vec{r}$, where $\vec{r}$ locates a lattice point. The diffusivity assigned to each lattice point is either the bulk or the GB diffusivity, namely D_B or D_{GB}, respectively, the latter a random variable drawn from the pdf, $p(D_{GB})$. To obtain $p(D_{GB})$, a connection between γ and D_{GB} is established by invoking an empirical relation due to Borisov [26–29] given by

$$\gamma(\psi) = \left(\frac{1}{2\alpha^2}\right)[k_B T ln(\eta) + \Delta Q(\psi)], \tag{4}$$

where α is the average atomic distance, η is (approximately) the ratio of the GB and bulk diffusional prefactors and ΔQ is the difference between the bulk and the GB diffusional activation energies. One then finds that, at temperature T,

$$D_{GB} \approx D_B exp(2\alpha^2\gamma(\psi)/k_B T), \tag{5}$$

where D_B is the bulk diffusivity and k_B is Boltzmann's constant [30]. For future use it is convenient to rewrite Eq. (4) as

$$\overline{\gamma} = \frac{\gamma(\psi)}{\gamma_0} = \frac{ln\left(\frac{D_{GB}}{D_B}\right)}{ln\left(\frac{D_{GB}^{max}}{D_B}\right)}, \tag{6}$$

where D_{GB}^{max} is the maximum GB diffusivity corresponding to a misorientation $\psi = \pi/4$. In our simulations, $D_B/D_0 = 9.16 \times 10^{-6}$, where D_0 is the bulk diffusional prefactor, and $\eta = 5$. This value for the bulk diffusivity was chosen to correspond to a system with a diffusional activation energy of 1.0 eV at a temperature of 1000 K.

Having assigned diffusivities to each lattice point, our approach employs a control-area based, finite-difference method to obtain the concentration field, $c(\vec{r})$, as a function of position, $\vec{r}$. For simplicity, we take the diffusivity, $D(\vec{r})$ to be an isotropic field that depends on $\vec{r}$. The determination of an effective diffusivity, D_{eff}, follows from a calculation of the steady-state flux. In particular, central-difference techniques [19] are employed to discretize the differential equation

$$\vec{\nabla} \cdot \left[D\left(\vec{r}\right)\vec{\nabla}c\left(\vec{r}\right)\right] = 0, \tag{7}$$

along with a tridiagonal matrix algorithm to obtain a numerical solution [31]. Dirichlet boundary conditions $c(y = 0) = 1$ and $c(y = \ell) = 0$ and Neumann conditions $(\partial c/\partial x)(x = 0) = (\partial c/\partial x)(x = \ell) = 0$ are imposed on the unit cell to obtain a unique solution (see Fig. 1).

After the solution converges to the steady-state concentration profile, $c_{ss}(\vec{r})$, the associated flux vector, $\vec{J}(\vec{r}) = -D(\vec{r})\vec{\nabla}c_{ss}(\vec{r})$, is obtained for each control area. The effective diffusivity is calculated by performing an areal average of the flux. One then obtains

$$D_{eff} = \ell\left\langle \vec{J}\left(\vec{r}\right)\right\rangle \cdot \hat{y}, \tag{8}$$

where the angle brackets denote an average over the control areas comprising the system [32]. To obtain statistically meaningful values for the effective diffusivity, the results are averaged over approximately 100 realizations of the microstructure for a given set of grain-orientation parameters.

3. Results

3.1. Simulations results

Consider first a grain-orientation pdf, $p(\phi)$, consisting of a single Gaussian (see Eq. (1)) having a standard deviation (i.e., width parameter) σ. As described above, by transformation of variables, one may construct two other pdfs, namely that for the GB energy, γ, and for the GB diffusivity, D_{GB}. Fig. 2a and b shows the pdfs for γ and D_{GB}, respectively, for $\sigma = 0.1$ while Fig. 3a and b shows the corresponding figures for $\sigma = 1.0$. For ease of comparison, the GB diffusivity is normalized by the bulk diffusivity, D_B. A comparison of Figs. 2a and 3a reveals that there is a higher fraction high-γ boundaries for $\sigma = 1.0$. This occurs since an increase in σ results in an increase in high-misorientation, and therefore high-γ, boundaries. As high-γ boundaries are also high-diffusivity interfaces (see Eq. (5)), the distribution in Fig. 3b contains many high-diffusivity GBs relative to that shown in Fig. 2b. Putting these results together, Fig. 4 shows the effective diffusivity, D_{eff}, as a function of σ. As is evident from the figure, D_{eff} increases with increasing σ until, for sufficiently large σ, it converges to the result obtained for a uniform pdf for $0 \le \phi \le \pi/2$ (dashed line). This result follows from the fact that, in the limit of small σ, grain misorientations and the corresponding GB energy are relatively small. Hence, from Eq. (5), the associated diffusivity is also small, leading to a relatively small D_{eff}. As σ increases, larger misorientations with larger concomitant GB diffusivities are produced, thereby leading to an increase in D_{eff}. Clearly, for relatively large values of σ, $p(\phi)$ becomes more like the uniform pdf and, hence, the observed plateau in Fig. 4.

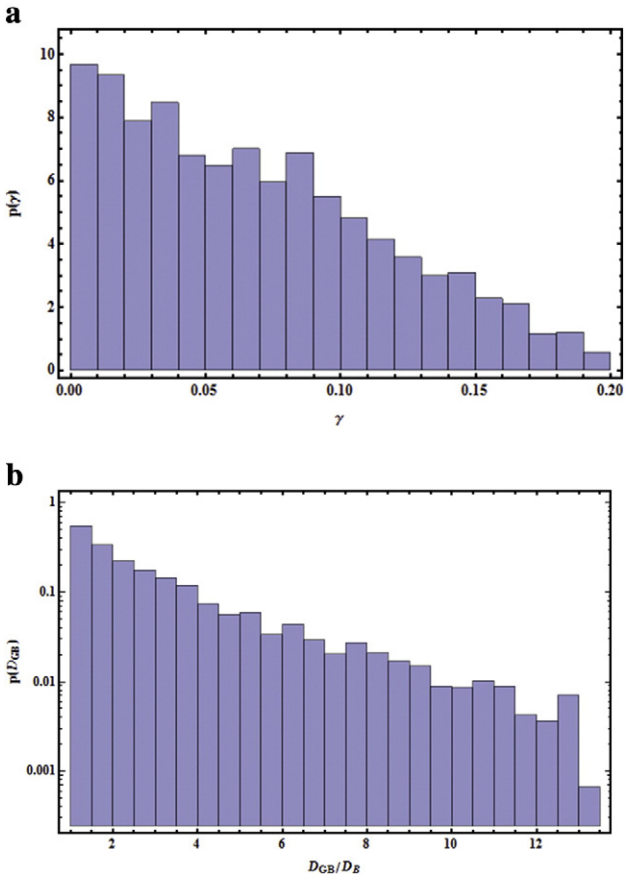

Fig. 2. a.) The probability density function, $p(\gamma)$, for the GB energy, γ, for a grain-orientation pdf consisting of a single Gaussian with width parameter $\sigma = 0.1$. b.) The probability density function, $p(D_{GB})$, versus the normalized GB diffusivity, D_{GB}/D_B, for a grain-orientation pdf consisting of a single Gaussian with width parameter $\sigma = 0.1$.

To represent a microstructure with a more complex texture, consider next a grain-orientation pdf comprising two Gaussians (see Eq. (2)) with peaks separated by Δ, having relative height λ, and each having the same width parameter σ. We are interested in the dependence of D_{eff} on the texture parameters Δ, λ and σ. Fig. 5 shows the double-peaked grain-misorientation pdf for this case and, for comparison, the pdf for a spatially random distribution of misorientations. For the latter pdf, the peak for small misorientations is higher because such misorientations can be created by drawing two grain orientations from the same peaked region of the grain-orientation pdf. The reason for the difference between these pdfs is that, in the former case, grain misorientations are not randomly distributed due to the crystallographic constraint that grains meet at triple junctions. VanSiclen has discussed the energetic consequences of this constraint in two recent publications [24].

The dependence of D_{eff}/D_B on Δ is shown in Fig. 6a for $\sigma = 0.05$ and $\lambda = 1$. The initial increase in D_{eff} is due to the creation of more high-misorientation boundaries as peak separation increases. D_{eff} reaches a maximum at $\Delta = \pi/4$ as $\gamma(\psi)$ is a maximum for the misorientation $\psi = \pi/4$ (45°). Fig. 6b shows the dependence of D_{eff}/D_B on relative peak height, λ for $\Delta = \pi/4$ and $\sigma = 0.05$. As is evident from the figure, there are, broadly speaking, two diffusive regimes. For small λ relatively large grain misorientations are dominant as grain orientations are often drawn from separate peaks. This dominance of larger misorientations results in a relatively large value for D_{eff}. The observed decrease in D_{eff} at large λ follows from the fact that larger values of λ favor sampling of orientations associated with the higher-peaked Gaussian and,

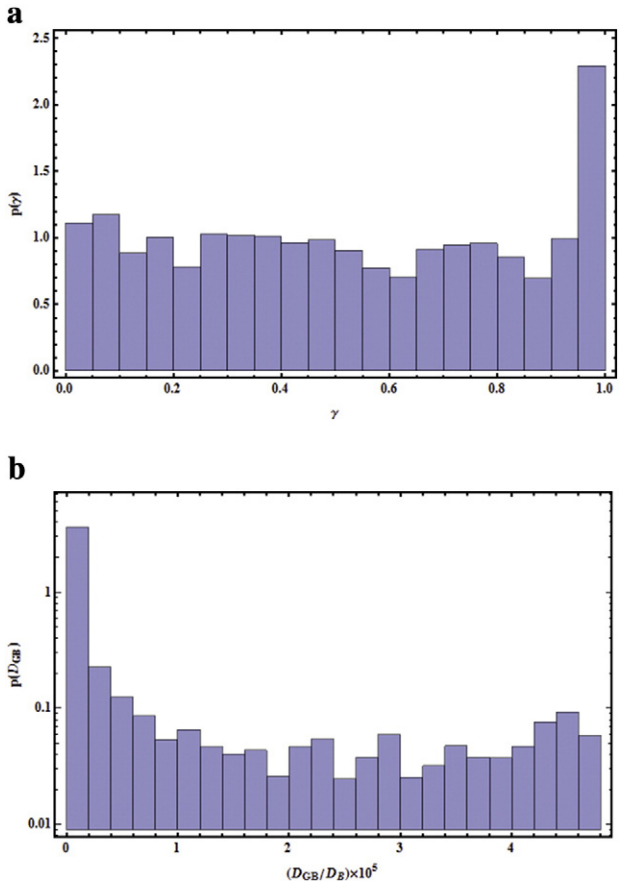

Fig. 3. The same as for Fig. 2, except for $\sigma = 1.0$.

thereby, the prevalence of low-angle grain boundaries. These low-angle boundaries are associated with smaller values of γ and, hence, smaller values of the effective diffusivity, D_{eff}. Finally, the dependence of D_{eff}/D_B on peak width, σ, is shown in Fig. 6c for $\Delta = \pi/4$ and $\lambda = 1$. The non-monotonic behavior of $D_{eff}(\sigma)$ exhibited in this figure can be understood as follows. For small σ, the sampling is dominated by large misorientations associated with orientations drawn from two well-separated peaks. As σ initially increases, there are larger misorientations associated with both peaks, leading to more high-angle boundaries and, therefore, an increase in D_{eff}. However, for somewhat larger values of σ, sampling tends to occur more often for a narrow range of ϕ associated with one peak, leading to an increase in low-angle boundaries and a

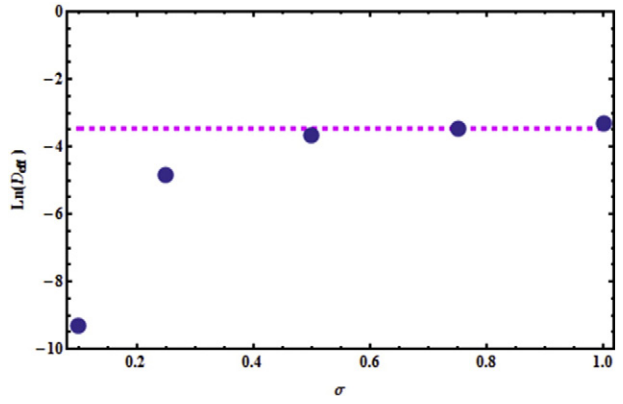

Fig. 4. The effective diffusivity, lnD_{eff}, as a function of the width parameter, σ, for a grain-orientation pdf consisting of a single Gaussian. The dashed line corresponds to D_{eff} for grain orientations distributed uniformly on $[0, \pi/2]$.

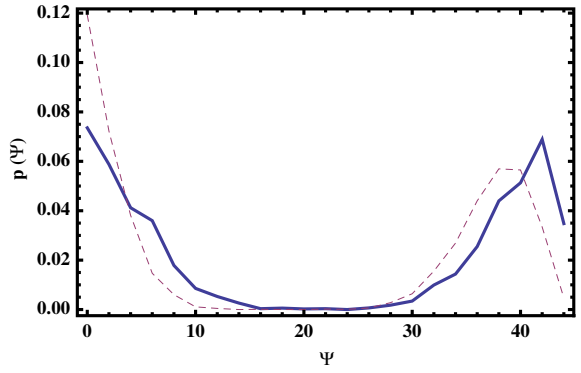

Fig. 5. The grain-misorientation pdf, $p(\psi)$ versus the grain misorientation, ψ, for the case used here in which the grain-orientation pdf comprises two Gaussians (solid line). For comparison, the pdf for a spatially random distribution of misorientations is also displayed (dashed line). For this case, $\Delta = \pi/4$, $\sigma = 0.07$ and $\lambda = 1.0$. The texture parameters Δ and σ control the relative proportion of low- and high-angle boundaries present in the microstructure.

decrease in D_{eff}. For relatively large values of σ, the peaks would overlap considerably and, in this limit, it is expected that D_{eff} will be nearly that associated with a uniform distribution of ϕ.

3.2. Effective medium theory

It is useful to obtain a semi-quantitative model to interpret the results presented in the previous section. In particular, we will construct a simplified description of the texture models described above and, from the corresponding pdfs, calculate an effective diffusivity. From this point of view, the grain-orientation, ϕ, and therefore the misorientation ψ, can be regarded as continuous random variables whose pdfs will dictate the effective diffusivity of the associated microstructure. Although it is possible to employ the truncated Gaussians used in the numerical calculations outline above, it is simpler to replace this function by the appropriate number of rectangular functions. Thus, if ϕ is uniformly distributed on the interval $[0, \sigma]$, then the associated grain-orientation pdf is given by

$$p(\phi) = \left(\frac{1}{\sigma}\right)\Theta(\phi)\Theta(\sigma-\phi), \tag{9}$$

where $\Theta(\phi)$ denotes a step function. As described in the Appendix A, if two random grain orientations, ϕ_1 and ϕ_2, are drawn independently from this uniform density, then one can calculate the pdf for the associated grain misorientation $\psi = |\phi_1 - \phi_2|$ and, using Eq. (3) and a transformation of variables, the pdf associated with the reduced GB energy $\overline{\gamma} = \gamma(\psi)/\gamma_0$. To compute the effective diffusivity with this model, it is necessary to determine first the pdf for the GB diffusivity. This is accomplished by employing the Borisov relation (Eq. (6)) and performing a change of variables to obtain $p(D_{GB})$. An expression for the pdf is given in the Appendix A.

Having obtained $p(D_{GB})$, one can now calculate D_{eff} using effective-medium theory. In this approach an effective diffusivity is obtained for an idealized model comprising diffusive elements, by analogy with the theory of electrical conduction in mixtures [33]. In particular, one assumes that there is a spectrum of GB diffusivities on a lattice, and that the system is outside the percolation regime. For the purposes of illustration, we will neglect here the contributions to D_{eff} from bulk sites. Following Kirkpatrick [33], one finds, for a square lattice, that

$$\int dD_{GB}\ \frac{D_{GB}-D_{eff}}{D_{GB}+D_{eff}}\ p(D_{GB}) = 0. \tag{10}$$

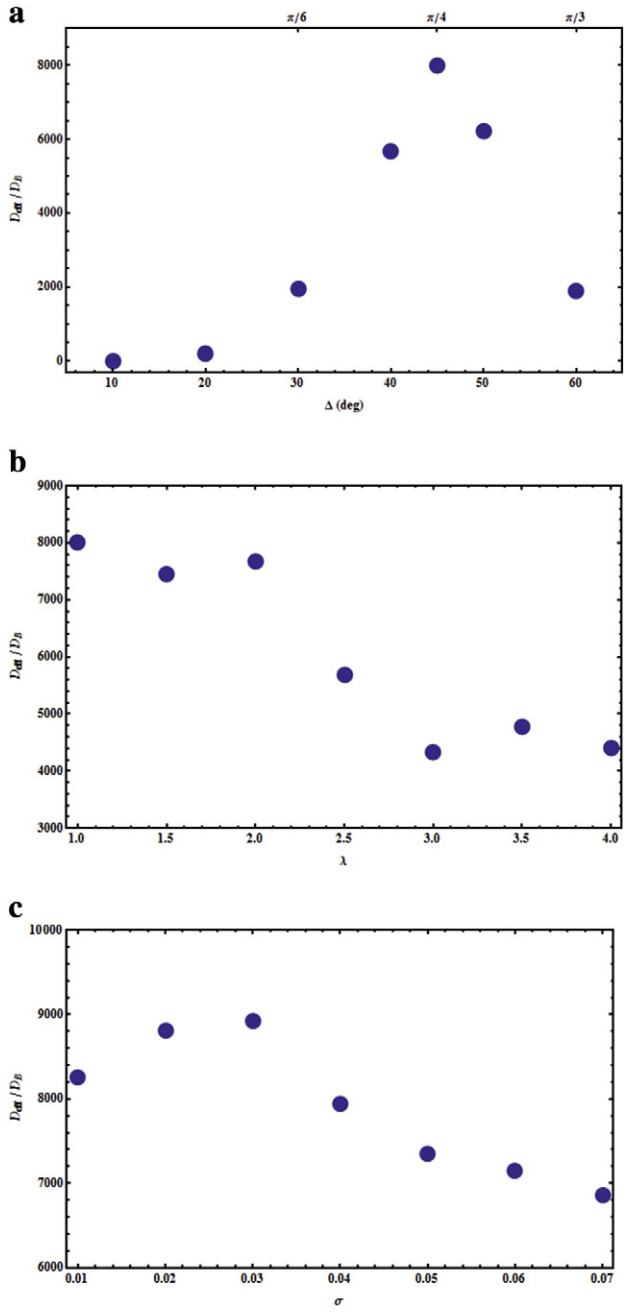

Fig. 6. a.) The dependence of the normalized effective diffusivity, D_{eff}/D_B, on peak separation, Δ, for the case in which the grain-orientation pdf consists of two Gaussians. For this case, $\sigma = 0.05$ and $\lambda = 1$. The maximum in D_{eff} at $\Delta = \pi/4$ corresponds to a maximum in the GB energy, $\gamma(\psi)$, at $\psi = \pi/4$. b.) The dependence of the normalized effective diffusivity, D_{eff}/D_B, on relative peak height, λ for the case in which the grain-orientation pdf consists of two Gaussians. The decrease in D_{eff} with increasing λ results from preferred sampling of the higher-peaked Gaussian. For this case, $\Delta = \pi/4$ and $\sigma = 0.05$. c.) The dependence of the normalized effective diffusivity, D_{eff}/D_B, on peak width, σ, for the case in which the grain-orientation pdf consists of two Gaussians. For this case, $\Delta = \pi/4$ and $\lambda = 1$.

This equation can be solved iteratively for D_{eff} using numerical integration upon substitution of D_{GB}.

As an illustration of this method, consider a textured microstructure with a grain-orientation pdf described by Eq. (9). Fig. 7 shows a plot of $ln[D_{eff}/D_{eff}(\sigma = \pi/2)]$ versus the width parameter, σ for this microstructure. As is evident from the figure, D_{eff} increases as σ increasing until reaching a limiting value of $D_{eff}(\sigma = \pi/2)$. This behavior is very similar to that seen in Fig. 4. While the two figures are qualitatively similar,

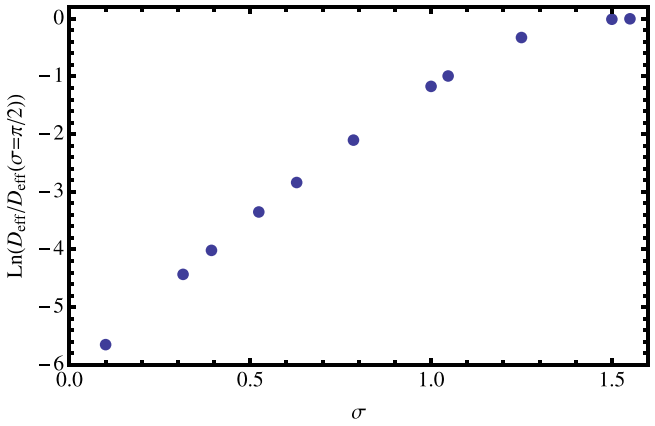

Fig. 7. The reduced diffusivity, lnD_{eff}/D_{eff}, $(\sigma = \pi/2)$ versus the width parameter, σ for a textured microstructure having a single grain-orientation peak. These results were obtained using effective-medium theory.

quantitative differences between them are due to several factors. These differences can be attributed, for example, to assumptions inherent in mean-field theory (e.g., ignoring spatial correlations among boundaries and detailed grain shape) that approximate the description of the model system and to the fact that, as stated above, the contribution of bulk sites to the diffusivity are, for simplicity, ignored in the mean-field treatment. Finally, the use of rectangular functions (see Eq. (9)) to approximate Gaussians will also lead to discrepancies between the curves in Figs. 4 and 7.

4. Discussion and conclusions

We have examined the impact of orientational anisotropy on diffusion at internal interfaces (i.e., grain boundaries) and, in particular, the role of preferred crystallographic orientation (i.e., texture) on mass transport in a polycrystal. From both computer simulation and effective medium theory, it was found that anisotropy has a significant impact on the effective diffusivity of an assemblage of grains. The impact of texture on the effective diffusivity was expressed in terms of basic shape features of the grain misorientation distribution, such as peak heights, widths, and separation. These shape features control the relative proportion of low- and high-angle boundaries and therefore, via the Borisov relation, the collective diffusion response of a polycrystal. Moreover, crystallographic constraints were shown to affect the grain misorientation distribution and, therefore, the effective diffusivity.

The results obtained here suggest several directions for study. One may, for example, wish to tailor a microstructure to obtain a particular range of effective diffusivities. From this work, it is evident that the grain-orientation pdf may be engineered so as to produce the desired distribution of boundary diffusivities. In particular, one can envision a reverse engineering strategy exploiting the methodology described here that would yield the desired results for a number of different textures. It would also be of interest to extend the results here to the percolation regime in which the connectivity of clusters of boundaries will determine observed properties. It is expected that effective medium theory will fail in this regime, and one may be limited to some degree to numerical investigations. As we have considered here two-dimensional microstructures, we would also like to examine the role of boundary variability in three-dimensional polycrystals. While one would expect qualitative similarities between the kinetics in two- and three-dimensions, quantitative differences may be expected due to topological differences associated with grain morphologies and grain connectivity.

Finally, as discussed above, our description of GB energetics in terms of grain misorientation alone is a simplification, and so it is of interest to include local GB orientation information in the description as well. Other authors have suggested approximate energy expressions [24]

that incorporate additional degrees of freedom associated with grain boundaries. These expressions can easily be incorporated into the numerical scheme for calculating effective diffusivity described here. In reality, of course, the situation is more complex. In particular, Rohrer and coworkers have shown that a knowledge of the full grain-boundary character distribution is important in determining energetics [34,35]. More generally, given the wealth of experimental data for GB energies as a function of the macroscopic GB degrees of freedom that is becoming available, it should be possible to formulate soon expressions for GB diffusivities in three-dimensional systems that incorporate this additional information. These research directions are the subject of ongoing studies.

Appendix A

We consider here a number of prototypical pdfs that highlight the main features of random and oriented grain distributions. For simplicity, we will employ a random, grain-orientation variable, ϕ, that is uniformly distributed on the interval $[0, \sigma]$. The associated probability density function (pdf) is then given by

$$p(\phi) = \left(\frac{1}{\sigma}\right)\Theta(\phi)\Theta(\sigma-\phi), \tag{11}$$

where $\Theta(\phi)$ denotes a step function.

Suppose that two independent, random grain orientations, ϕ_1 and ϕ_2, are drawn such that their joint density $p(\phi_1, \phi_2) = p(\phi_1)p(\phi_2)$. One can then define the orientation difference $\Psi = \phi_1 - \phi_2$ and, via a transformation of variables [36], the associated pdf is

$$\begin{aligned}\tilde{p}(\Psi) &= \int_{-\infty}^{\infty}\int_{-\infty}^{\infty} d\phi_1 d\phi_2 \;\; p(\phi_1)p(\phi_2) \;\; \delta(\Psi-\phi_1+\phi_2) \\ &= \int_{-\infty}^{\infty} d\phi_2 \;\; p(\Psi+\phi_2)p(\phi_2).\end{aligned} \tag{12}$$

One then finds that

$$\tilde{p}(\Psi) = \left(\frac{1}{2\sigma^2}\right)(|\Psi-\sigma| + |\Psi+\sigma| - 2|\Psi|), \tag{13}$$

and that, for the misorientation, $\psi = |\Psi|$, the associated pdf is

$$p'(\psi) = \left(\frac{2}{\sigma^2}\right)(\sigma-\psi) \;\; \Theta(\psi)\Theta(\sigma-\psi). \tag{14}$$

(For notational simplicity, we will henceforth denote all pdfs with the function p.) We note here that, as discussed in the text, the assignment of random orientations to a microstructure results in subtle misorientation correlations owing to crystallographic constraints.

We next wish to obtain the pdf associated with the grain-boundary energy $\gamma = \gamma_0 sin(2\psi)$ (Eq. (3)). Taking $\overline{\gamma} = \gamma/\gamma_0$, one has that

$$p(\overline{\gamma}) = \int_{-\infty}^{\infty} d\psi \;\; p(\psi) \;\; \delta(\overline{\gamma} - sin(2\psi)). \tag{15}$$

It is convenient here to employ the delta function expansion [37] for $0 \le a \le \pi/2$

$$\delta(\overline{\gamma} - sin(2\psi)) = \frac{1}{2\sqrt{1-\overline{\gamma}^2}} \;\; [\delta(\psi-\psi_0) + \delta(\psi-\psi_1)], \tag{16}$$

where $\psi_0 = (1/2)sin^{-1}(\overline{\gamma})$ and $\psi_1 = \pi/2 - (1/2)sin^{-1}(\overline{\gamma})$. Upon substituting Eq. (16) into Eq. (15) and integrating, one obtains, for $0 \le \sigma \le \pi/4$,

$$p(\overline{\gamma}) = \left(\frac{1}{\sigma^2}\right) \;\; \frac{1}{\sqrt{1-\overline{\gamma}^2}} \;\; \left[\sigma - \frac{1}{2}sin^{-1}(\overline{\gamma})\right]\Theta(\overline{\gamma})\Theta(sin(2\sigma)-\overline{\gamma}), \tag{17}$$

and, for $\pi/4 < \sigma \le \pi/2$,

$$p(\overline{\gamma}) = \begin{cases} \left(\frac{1}{\sigma^2}\right) \;\; \frac{1}{\sqrt{1-\overline{\gamma}^2}} \;\; \left[\sigma - \frac{1}{2}sin^{-1}(\overline{\gamma})\right]\Theta(\overline{\gamma})\Theta(sin(2\sigma)-\overline{\gamma}), \\ \left(\frac{1}{\sigma^2}\right) \;\; \frac{1}{\sqrt{1-\overline{\gamma}^2}} \;\; \left[2\sigma - \frac{\pi}{2}\right] \;\; \Theta(\overline{\gamma}-sin(2\sigma))\Theta(1-\overline{\gamma}). \end{cases} \tag{18}$$

Finally, consider the pdf corresponding to a strong texture having two primary grain orientations separated in angle by Δ. For simplicity, we take the heights of the two peaks to be the same (i.e., $\chi = 1$). In this case,

$$p(\phi) = \left(\frac{1}{2\sigma}\right)[\Theta(\phi)\Theta(\sigma-\phi) + \Theta(\phi-\Delta)\Theta(\sigma+\Delta-\phi)], \tag{19}$$

and the associated misorientation distribution is given by

$$p(\psi) = \left(\frac{1}{\sigma^2}\right)\left[(\sigma-\psi) \;\; \Theta(\psi)\Theta(\sigma-\psi) + \frac{1}{4}(|\sigma+\Delta-\psi| + |\sigma-\Delta+\psi| - 2|\Delta-\psi|)\right]. \tag{20}$$

This misorientation distribution has two peaks of unequal height. This difference in peak height arises because two similar orientations are sampled more often than two dissimilar orientations.

References

[1] G. Ayrault, G. Ehrlich, J. Chem. Phys. 60 (1974) 281.
[2] D.W. Bassett, P.R. Webber, Surf. Sci. 70 (1978) 520.
[3] G. Antczak, G. Ehrlich, Surf. Sci. Rep. 62 (2007) 39.
[4] D. Turnbull, R. Hoffman, Acta Metall. 2 (1954) 419.
[5] R.W. Balluffi, Metall. Trans. A 13A (1982) 2069.
[6] J. Herbeuval, M. Biscondi, C. Goux, Mem. Sci. Rev. Met. 70 (1973) 39.
[7] C.-S. Kim, Y. Hu, G.S. Rohrer, V. Randle, Scr. Mater. 52 (2005) 633.
[8] U.F. Kocks, C.N. Tome, H.-R. Wenk, Texture and Anisotropy: Preferred Orientations in Polycrystals and Their Effect on Materials Properties, Cambridge University Press, Cambridge, UK, 1998.
[9] B.A. Gnesin, Y.P. Yashnikov, in: M.P. Anderson, A.D. Rollett (Eds.), Simulation and Theory of Evolving Microstructures, TMS, Warrendale, PA, 1990.
[10] Y. Chen, C.A. Schuh, Acta Mater. 54 (2006) 4709.
[11] L. Li, S. Holland, Nanomater. Energy 3 (2014) 139.
[12] M.M. Moghadam, J.M. Rickman, M.P. Harmer, H.M. Chan, J. Appl. Phys. 117 (2015) 045311.
[13] One exception is the recent work of Mohebi-Moghadam *et al.* that also considers a spectrum of boundary diffusivities that are deduced from experiment [12].
[14] J.K. Mackenzie, Biometrika 45 (1958) 229.
[15] E.A. Holm, G.N. Hassold, M.A. Miodownik, Acta Mater. 49 (2001) 2981.
[16] O. Engler, V. Randle, Introduction to Texture Analysis: Macrotexture, Microtexture and Orientation Mapping, Taylor and Francis Group, Boca Raton, FL, 2010.
[17] Q. Du, V. Faber, M. Gunzburger, SIAM Rev. 41 (1999) 637.
[18] A. Okabe, B. Boots, K. Sugihara, Spatial Tessellations: Concepts and Applications of Voronoi Diagrams, John Wiley, New York, 1992.
[19] W.H. Press, B.P. Flannery, S.A. Teukolsky, W.T. Vetterling, Numerical Recipes: The Art of Scientific Computing, Cambridge University Press, New York, 1989.
[20] G.H. Givens, J.A. Hoeting, Computational Statistics, John Wiley and Sons, Hoboken, NJ, 2013.
[21] J.P. Hirth, J. Lothe, Theory of Dislocations, Krieger, Malabar, Florida, 1992.
[22] J.M. Rickman, J. Viñals, R. LeSar, Philos. Mag. 85 (2005) 917.
[23] D. Moldovan, D. Wolf, S.R. Phillpot, A.J. Haslam, Philos. Mag. A 82 (2002) 1271.
[24] C.D. Van Siclen, Acta Mater. 55 (2003) 983.
[25] C.DeW. Van Siclen, Phys. Rev. B 73 (2006) 184118.
[26] V.T. Borisov, V.M. Golikov, G.V. Scherbedinskiy, Phys. Met. Metallogr. 17 (1964) 80.
[27] P. Guiraldenq, P. Poiret, Mem. Sci. Rev. Met. 70 (1973) 715.
[28] T.-F. Chen, G.P. Tiwari, Y. Iijima, K. Yamauchi, Mater. Trans. 44 (2003) 40.
[29] J. Pelleg, Philos. Mag. 14 (1966) 595.
[30] The parameter η also involves the segregation coefficient, the grain-boundary width and the interatomic spacing.
[31] S. Patankar, Numerical Heat Transfer and Fluid Flow, CRC Press, 1980.
[32] S. Prager, J. Chem. Phys. 33 (1960) 122.
[33] S. Kirkpatrick, Rev. Mod. Phys. 45 (1973) 574.
[34] S. Ratanaphan, Y. Yoon, G.S. Rohrer, J. Mater. Sci. 49 (2014) 4938.
[35] G.S. Rohrer, J. Li, S. Lee, A.D. Rollett, M. Groeber, M. Uchic, Mater. Sci. Technol. 26 (2010) 661.
[36] S. Chakraborty, Appl. Appl. Math. (2008) 42.
[37] G.B. Arfken, H.J. Weber, Mathematical Methods for Physicists, Sixth Ed. Elsevier, New York, 2005.